Original Research

Measurement and analysis of the performance of photovoltaic modules under shaded conditions in an Algerian coastal region

Abderahim BOUSSAID [4], **Abdelkader AISSAT** [1,2,5,*], **Zoubeyr SMARA** [1,3], **Maamar DAHBI** [4], **Samuel DUPONT** [5]

[1] LATSI Laboratory, University Blida 1, Algeria;

[2] University of Ahmed Daria, 01.000, Algeria;

[3] Unité de développement des équipements solaires, UDES/Centre de développement des énergies renouvelables, CDER, 42415. Tipaza, Algérie;

[4] Laboratory for the Development of Renewable Energies and their Applications in Saharan Areas (LDERAS) Tahri Mohammed Bechar University, Algeria;

[5] Institute of Electronics, Microelectronics and Nanotechnology (IEMN), UMR CNRS 8520, University of sciences and Technologies of Lille 1, Avenue Poincare, 60069, 59652 Villeneuve of Ascq, France.

* Correspondence: sakre23@yahoo.fr

Received: January 14, 2026; Accepted: February 10, 2026

Abstract: Shading of photovoltaic (PV) panels presents a critical challenge in the building and residential sectors, as it can influence the reliability and performance of PV systems. To improve the efficiency of Buildings Integrated Photovoltaic (BIPV) applications, it is essential to analyze the effect of shading and implement appropriate solutions to ensure optimal energy production. In this context, an experimental study is conducted in this paper to investigate the impact of shading location on the power output of PV modules. The results demonstrated that power losses caused by horizontal shading are significantly greater than those resulting from vertical shading, highlighting the importance of managing shading to optimize systems performance. Besides, within the same string, the electrical behavior of a PV module subjected to random shading tends to reflect that of the most heavily shaded cell. This occurs because the most shaded cells limit the module's power output, thereby affecting the performance of the entire string.

Keywords: shading, hot-spot, bishop model, thermal stress, faults, solar cells.

1. Introduction

Currently, the construction sector ranks as one of the most energy-intensive and environmentally harmful industries worldwide, contributing to more than 30% of greenhouse gas emissions and surpassing 35% of the overall energy consumption in numerous countries [1,2]. As energy demand from buildings continues to rise, addressing this challenge has become a key focus for both governments and professionals in the industry, emphasizing the need to lower energy consumption in the building sector. This can be achieved through the development and integration of reliable MPPT systems and improved energy management in current structures [3,4], as well as a significant overhaul of design approaches for new constructions, incorporating sustainable practices and renewable energy sources [5-7]. The integration of renewable energy sources, particularly PV energy in buildings, is a vital component of the energy transition, driven by its cost-effectiveness and its potential to produce clean energy and lessen dependence on fossil fuels.

Shading of PV panels presents a critical challenge in residential applications. This issue has been noted in various installations, including the German program "1000 Solar Roofs PV," which reported that more than 40% of its installations were affected by this problem [8,9]. The presence of shading on PV modules can be a major barrier to their effectiveness, as it restricts the solar

irradiation that the PV cells can capture, thereby reducing overall energy production. Research findings from [10] indicate that partial shading can significantly diminish the efficiency of a module, thus impacting the overall energy performance of an installation.

Another impact of shading is the formation of a non-uniform irradiation distribution on the modules, which may cause mismatch losses. The shading impacts the cells in series differently, preventing them from achieving their optimal operating points and resulting in a loss of current. In severe instances, this inconsistency can lead to the formation of hot spots, posing a risk of damage to the PV cells. In response to the shading effects on PV modules, various technical solutions have been proposed, notably the use of bypass diodes. These diodes allow for the diversion of current around shaded cells, which helps to reduce the impact on energy production in a string of panels. A recent investigation revealed that the use of bypass diodes in PV panel systems substantially reduces efficiency loss due to localized shading and prevents thermal damage caused by hot spots [11-13].

In this paper, we will conduct an in-depth exploration of the effects of shading on PV modules, highlighting the significance of bypass diodes in determining their electrical efficiency. Additionally, we will present experimental data that highlights the relationship between shading percentage and the typical performance curve of PV modules, along with its effects on energy efficiency. The analysis reveals that energy output may decrease as a consequence of partial shading on a module. The experiments were conducted in Bou-Ismail, a coastal area in Algeria, located in North Africa, to examine the impact of shading and local weather conditions on the electrical performance of photovoltaic systems.

2. Mathematical modeling of shading

There are different types of solar cell models, among them, the single diode model being the most prevalent in the literature. This model is used to derive the I-V curve and to analyze the behavior of PV cells when they are exposed to a steady distribution of irradiation [14-16].

Shading on PV modules leads to the emergence of negative voltages across the impacted cells, which behave as receivers [17]. The single diode model referenced earlier is inadequate for describing the reverse operation of these cells. To resolve this issue, a variety of alternative models have been proposed with most integrating the avalanche effect into traditional modeling approaches [18,19]. The model put forth by Bishop [20] is one of the most referenced in the field, showing a satisfactory match with experimental observations. It includes an additional term to describe the avalanche effect, as indicated in equation 1.

$$I = \underbrace{I_{ph} - I_d\left[e^{\frac{q(V+I.R_S)}{nkT}} - 1\right] - \frac{V+IR_s}{R_{sh}}}_{forward-bias-range} - \underbrace{\frac{a(V+IR_s)}{R_{sh}}\left(1 - \frac{V+IR_s}{V_{Br}}\right)^{-m}}_{reverse-bias-range} \qquad (1)$$

With I_{Ph}, I_d, q, n, k, T, R_s and R_{sh} are the parameters of the single diode model, a is the correction factor (Ω^{-1}), V_{Br} is the avalanche voltage in volts and m is breakdown factor.

The equivalent circuit associated with the Bishop model is depicted in Figure 1.

The integration of this model into a model printing program allowed us to generate the *I-V* characteristic curve of the PV cell across the full voltage spectrum.

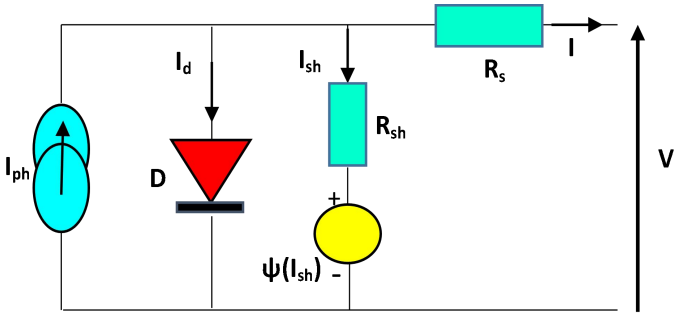

Figure 1. The equivalent circuit associated with the Bishop model.

The three operating quadrants are delineated in Figure 2.

- Quadrant 1: This indicates that the PV cell is functioning as a receiver. This situation arises when the illumination is unevenly distributed across a branch of the cell.
- Quadrant 2: where the PV cell acts as a generator.
- Quadrant 3: where the PV cell functions as a receiver. This scenario may occur when several modules are linked in parallel or when a load directly connected can alternate between receiving and generating modes.

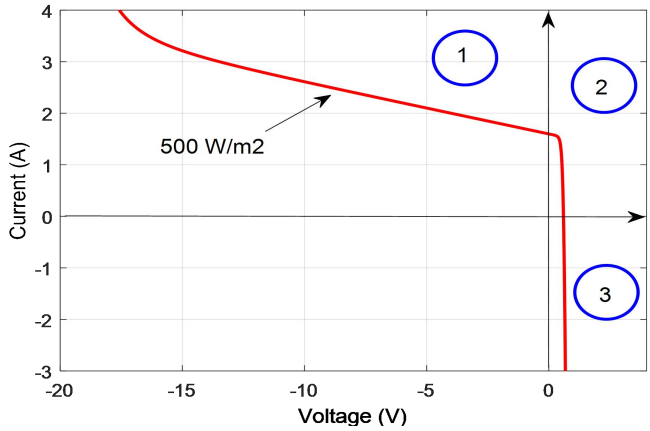

Figure 2. I-V curve of the solar cell over the entire voltage range.

The model for a series-connected module of 'N_S' cells can be generalized in the following manner:

$$I = I_{ph} - I_d\left[e^{\frac{q\left(\frac{V}{N_S}+IR_S\right)}{nkT}} - 1\right] - \frac{1}{R_p}\left(\frac{V}{N_S} + IR_s\right) - a\left(\frac{V}{N_S} + IR_s\right)\left(1 - \frac{V/N_S+IR_s}{V_{Br}}\right)^{-m} \quad (2)$$

In order to determine the *I-V* characteristic of a PV module featuring a shaded cell, we need to address the following equations:

$$I = I_1 + I_2 \quad (3)$$
$$V = V_1 + V_2 \quad (4)$$

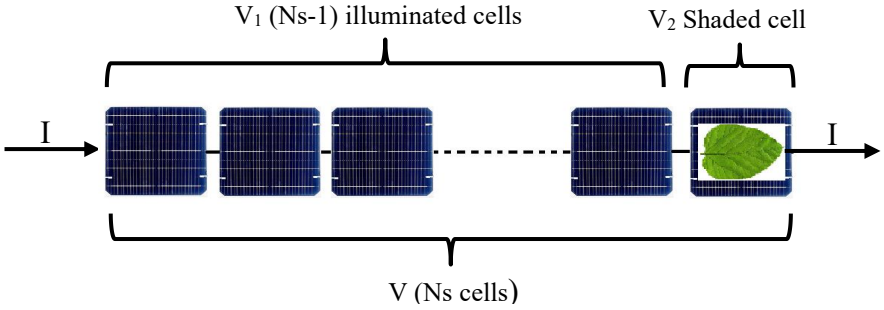

Figure 3. Synoptic of a partially shaded string

Such as:

$$I_1 = I_{ph} - I_d\left[e^{\frac{qb}{nkT}} - 1\right] - \frac{b}{R_p} - ab\left[1 - \frac{b}{V_{Br}}\right]^{-m} \quad (5)$$

$$I_2 = I_{ph} - I_d\left[e^{\frac{qc}{nkT}} - 1\right] - \frac{c}{R_p} - ac\left[1 - \frac{c}{V_{Br}}\right]^{-m} \quad (6)$$

where:

$$b = \frac{V_1}{N_s - 1} + IR_s \quad (7)$$

$$c = V_2 + IR_s \quad (8)$$

With V_1 and V_2 are the voltage of unshaded and shaded cells, respectively, and q is the electron charge. We developed a program in the Model printing environment to address this system of equations. The simulations were down at the standard conditions (G= 1000 W/m² and T=25°C) is illustrated in Figure 4. The *I-V* characteristics depicted in Fig. 5 are derived from different segments of a partially shaded PV module, where the shading percentage is set at Q = 30% (or a shading transmittance f_s= 70%). The findings indicate that the *I-V* characteristic of 35 normal cells is better than that of 36 cells, which has a shaded cell, as shown by the power dissipation in the latter.

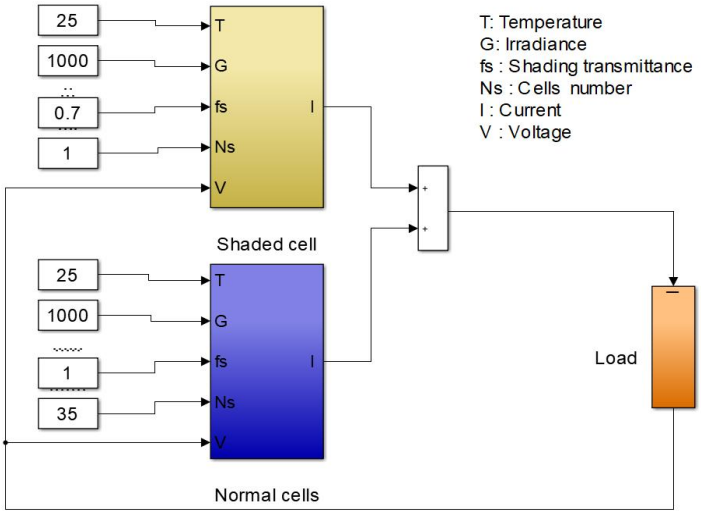

Figure 4. Model of a 36-cell PV module with a shaded cell in SIMULINK environment.

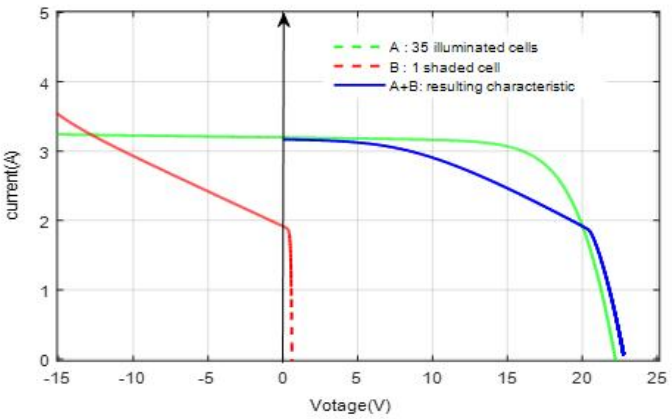

Figure 5. I-V characteristic of a 36-cell PV module with one cell shaded.

2.1. Effect of shading percentage

The shading effect has a direct impact on the photogenerated current I_{ph}, which in turn affects the power output in a proportional manner.

$$I_{ph.} = I_{SC-STC}\left(\frac{G}{1000}\right)f_s \qquad (9)$$

Where G is the irradiance, $I_{SC\text{-}STC}$ is the short circuit current at STC, f_s is the shading transmittance which varies between 0 to 1 and Q is the shading percentage defined by:

$$Q=1-f_s \qquad (10)$$

2.2. Bypass diode protection

To avoid shading problems, we need to connect a bypass diode referred to D_p, in parallel with a basic series group of cells. The immediate activation of this parallel diode upon the application of reverse voltage at the terminals of the group restricts the voltage to the direct conduction voltage V_D, of the selected diode, while the power dissipated is calculated as (I xV_D) (Figure 6. a).It should be emphasized that the number of cells within an elementary cells group is selected to ensure that the avalanche voltage does not exceed the specifications of the cell technology, with silicon cells typically ranging under 30 cells by bypass diode [21].Many modules available on the market today are equipped with parallel diodes for reverse voltage protection. The shadow effect can create two distinct Maximum Power Points (MPPs), which depend on the level of shading (Figure 6.b). The maximum point among these is generally random.

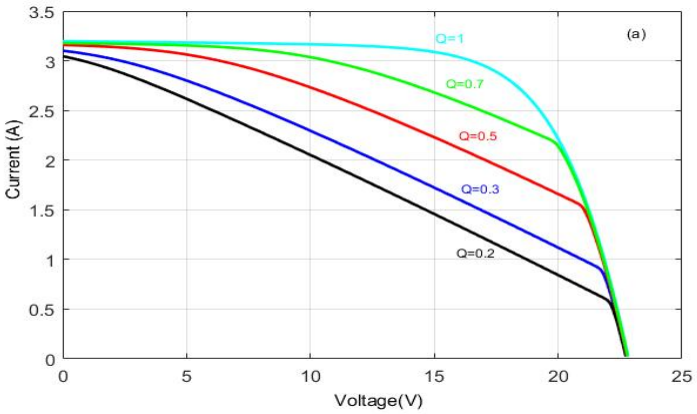

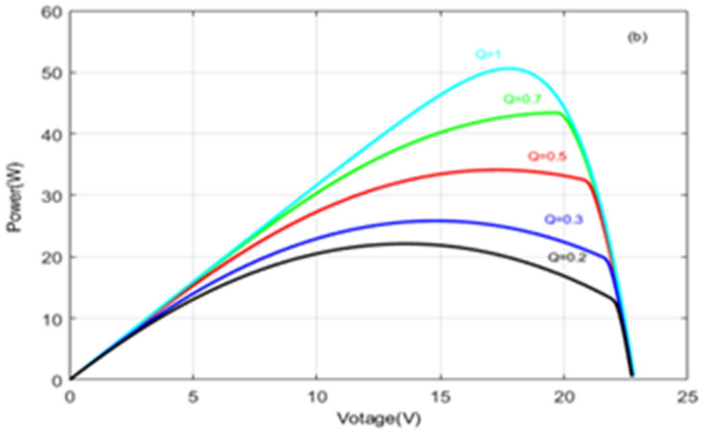

Figure 6. Displays the I-V and P-V characteristics for a 36-cell module, focusing on the behavior of one cell that is shaded at multiple shading percentages: a). I-V and b). P-V.

Figure 7 depicts the effect of shadowing on the *I-V* and *P-V* characteristics of a PV module that is safeguarded by two diodes. The influence of bypass diodes on the *I-V* and *P-V* characteristics of a module is contingent upon the extent of shading. Bypass diodes redirect current away from shaded sections of the module, thereby averting the formation of hot spots. In scenarios where the module experiences partial shading, a multi-peaked *I-V* curve is observed. Nonetheless, the effectiveness of bypass diodes is significantly influenced by the degree of shading present. At shading levels under 20%, the impact of the diodes is limited, resulting in low power loss and a minor effect on the *P-V* curve. In contrast, as shading increases, the effectiveness of the bypass diodes becomes more evident. However, even with these diodes, extensive shading across the cells can lead to substantial power loss.

In Figure 7 (a and b) the influence of bypass diodes on the *I-V* and *P-V* characteristics of a protected photovoltaic module is presented, highlighting different levels of shadi

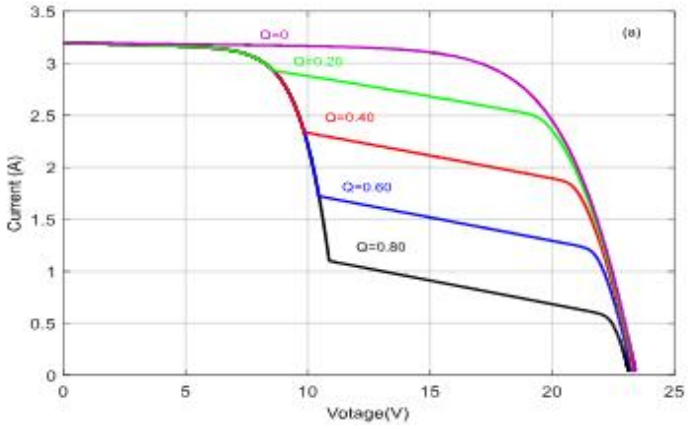

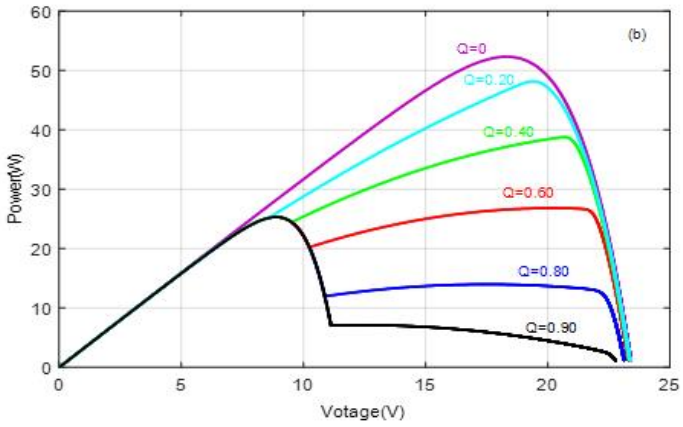

Figure 7. Influence of bypass diodes on the electrical characteristics of PV modules for different levels of shading a). I-V and b). P-V.

The impact of varying numbers of bypass diodes on the *I-V* and *P-V* characteristics of a PV module is depicted in Figure 8. An increase in the number of bypass diodes leads to a reduction in the number of isolated cells, resulting in higher power output for the module, which consequently drives up its price significantly.

Our analysis indicates that increasing the number of bypass diodes allows for more effective isolation of shaded regions, thereby minimizing the adverse effects on other cells within the module and enhancing the *I-V* and *P-V* characteristics. The presence of multiple bypass diodes leads to increased current levels and enhanced stability of maximum power output, even when partial shading occurs. The greater the number of bypass diodes, the better the module can sustain optimal performance, thereby reducing losses associated with shading. Nevertheless, incorporating several bypass diodes significantly raises the cost of the modules.

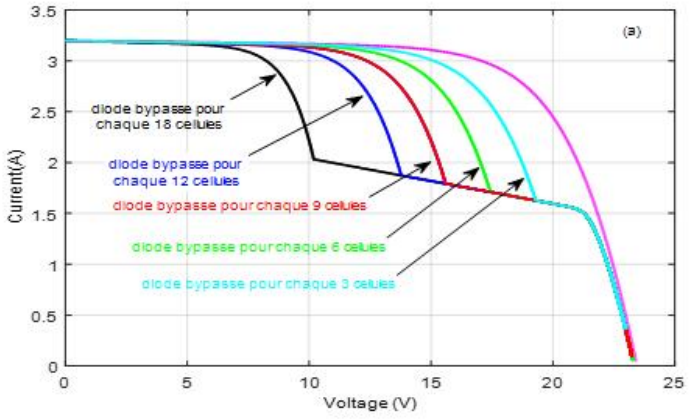

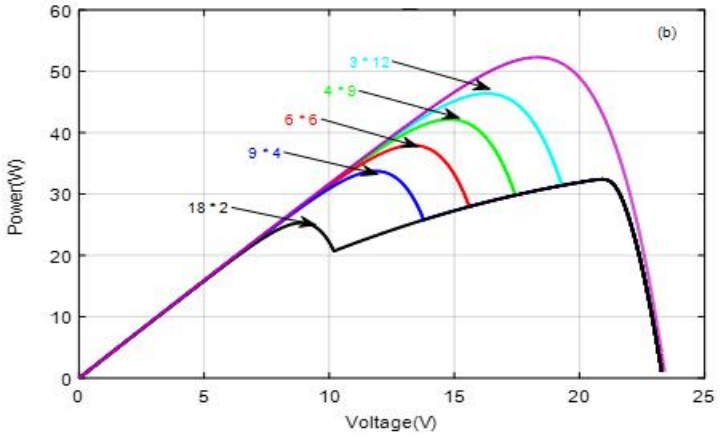

Figure 8. The influence of the quantity of bypass diodes on the power-voltage characteristics of a photovoltaic module.

3. Power losses caused by the partial shading effect

This section examines how shading profiles affect the electrical performance of PV modules. Various shading conditions, including both partial and total shading, were implemented on the modules to assess their impact on the *I-V* and *P-V* curves. A series of experiments were conducted to investigate these effects, and the findings are detailed in the following sections.

3.1. Shading a single cell with different percentages

In this experiment, a 135W polycrystalline PV module composed of 36 cells was utilized, with one cell subjected to varying degrees of shading (Q=20 to 100%). The main characteristics of the PV module used in the study are mentioned in table.1 and the various shading levels analyzed are illustrated in Figure 9. Figure 10 illustrates the characteristics derived for each shading level, with Q denoting the percentage of shading. The impact of shading percentage on the electrical performance of the module is distinctly noticeable, especially concerning the power curve. Specifically, the power output from the module diminishes in direct proportion to the amount of shading applied to the cell. When a cell is fully shaded (100%), the bypass diode facilitates the diversion of current around this section; however, the power loss is still considerable, amounting to approximately 50% of the maximum power output that the module could achieve without any shading. This reduction in performance underscores the detrimental effect of shading on the efficiency of PV modules.

The electrical properties of the module employed in the study.

Table 1. The electrical properties of the module employed in the study.

Characteristics	Detail
Cell type	Polycrystalline
Rated Power (P_{max})	135 Wp
Voltage at Maximum Power (V_{mpp})	17.50 V
Current at Maximum Power (I_{mp})	7.71 A
Open Circuit Voltage (V_{oc})	22.30 V
Short Circuit Current (I_{sc})	8.20 A
Number of bypass diodes	02
NOCT	(45±2)°C

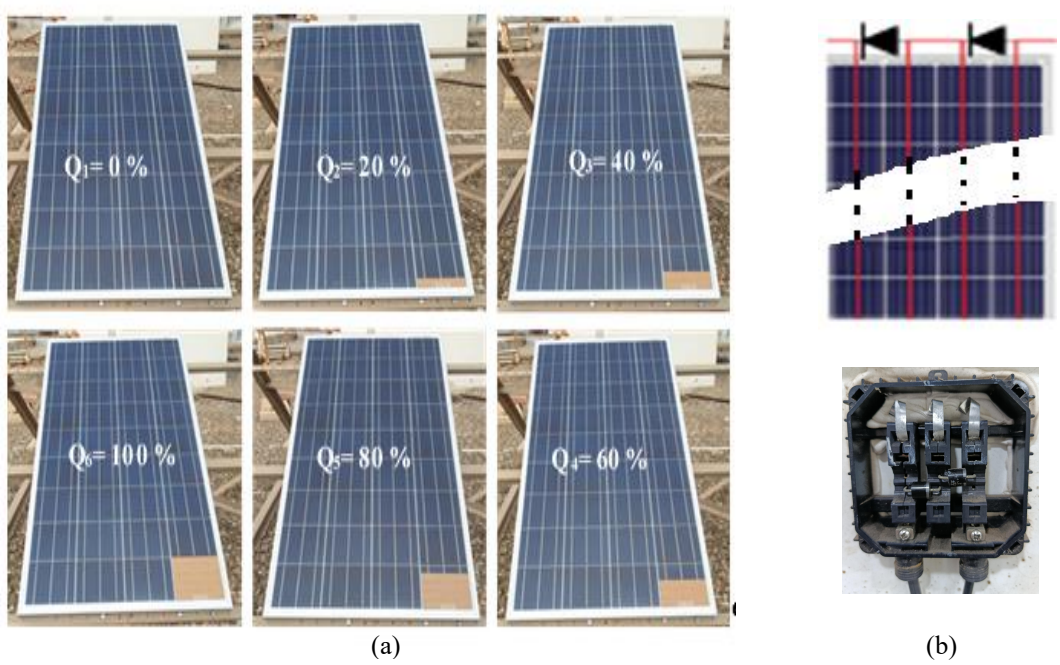

Figure 9. (a) Shading levels considered for PV cell, (b) Bypass diodes position in the PV module.

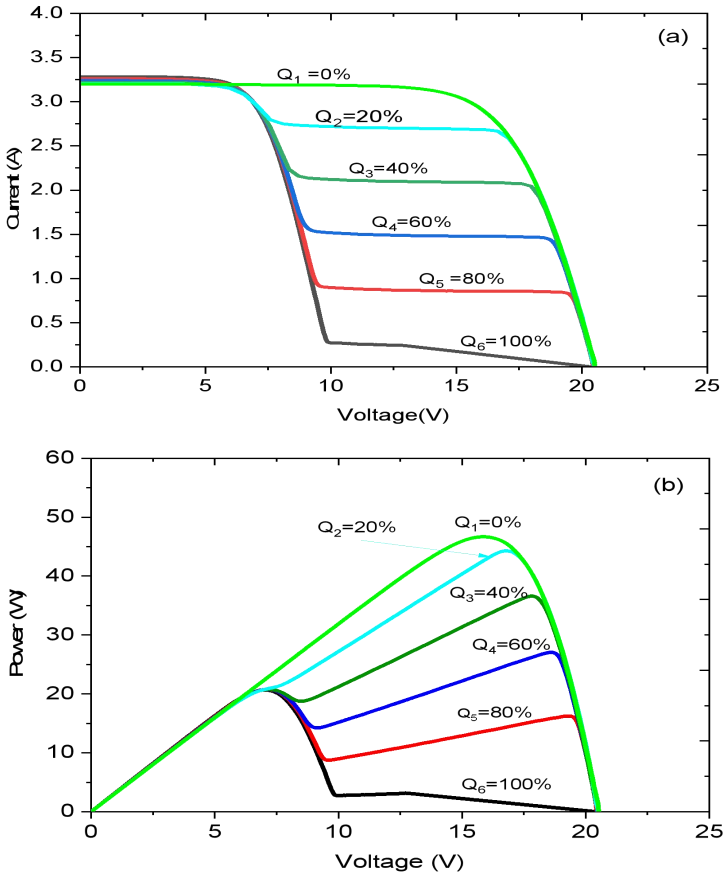

Figure 10. Illustrates the electrical characteristics corresponding to each level of shading analyzed: a). I-V and b). P-V.

3.2. Shading multiple cells in series

The objective of this test was to compare the impact of shading on a single photovoltaic cell with that exerted on several cells connected in series with it, ranging from one to nine shaded cells. The different experimental configurations are illustrated in Figure 11. The electrical characteristics measured for each of these configurations are presented in Figure 12.

Figure 11. Configuration considered for comparison.

A slight difference is observed between the behavior of a single shaded cell and that of nine (09) fully shaded cells. This difference is mainly evident in the unusable area of the I-V curves obtained. Analysis of the results shows that partial shading of several cells in series results in effects similar to those observed when a single cell is fully shaded. In other words, even when up to nine cells are affected by shading, the overall electrical characteristics of the module vary only slightly compared to the case of a single shaded cell. We observe that the shading effect on the maximum power of the panel is quite significant. Our measurement indicates that the maximum power at case 9 decreases from the reference power of 39.71W, meaning that shading reduces the maximum power by 53.31%.

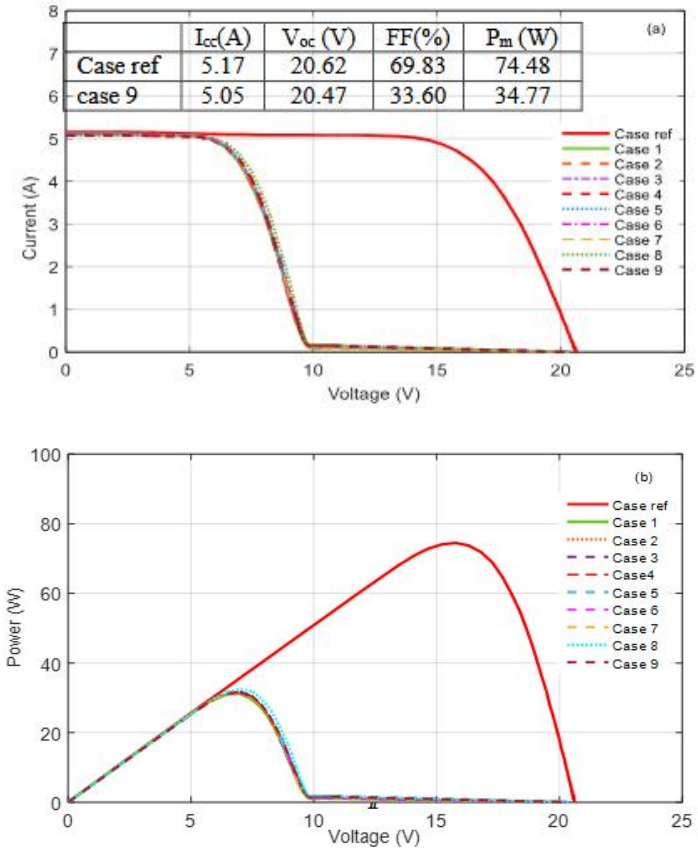

Figure 12. Characteristics obtained for the comparison considered: a). I-V and b). P-V.

3.3. Shading multiple cells in different parts of the PV module

3.3.1. Vertical shading

In this experiment, eight scenarios were analyzed. The shading position was adjusted following the acquisition of the characteristic curve for each scenario examined. Figure 13 depicts the various cases that were evaluated. The findings from this test show comparable results in some scenarios, which are arranged according to the identified similarities. Figure 14 depicts the attributes of the PV module classified based on these similarities for the eight cases examined. Figure 14 (a and b) illustrates that when vertical shading affects a cluster of cells within the same "string" (which has a single bypass diode connected in parallel), the characteristic curve exhibits stairs. This phenomenon occurs because the bypass diode activates, enabling the shaded cells to be bypassed, thereby interrupting the curve's continuity. Conversely, as illustrated in Figure 14. c, when vertical shading uniformly impacts all cells within the module, the characteristic curve remains continuous. This is due to the shading being uniform, which prevents any asymmetrical behavior in the diodes. This examination underscores the influence of shading on the overall efficiency of PV modules.

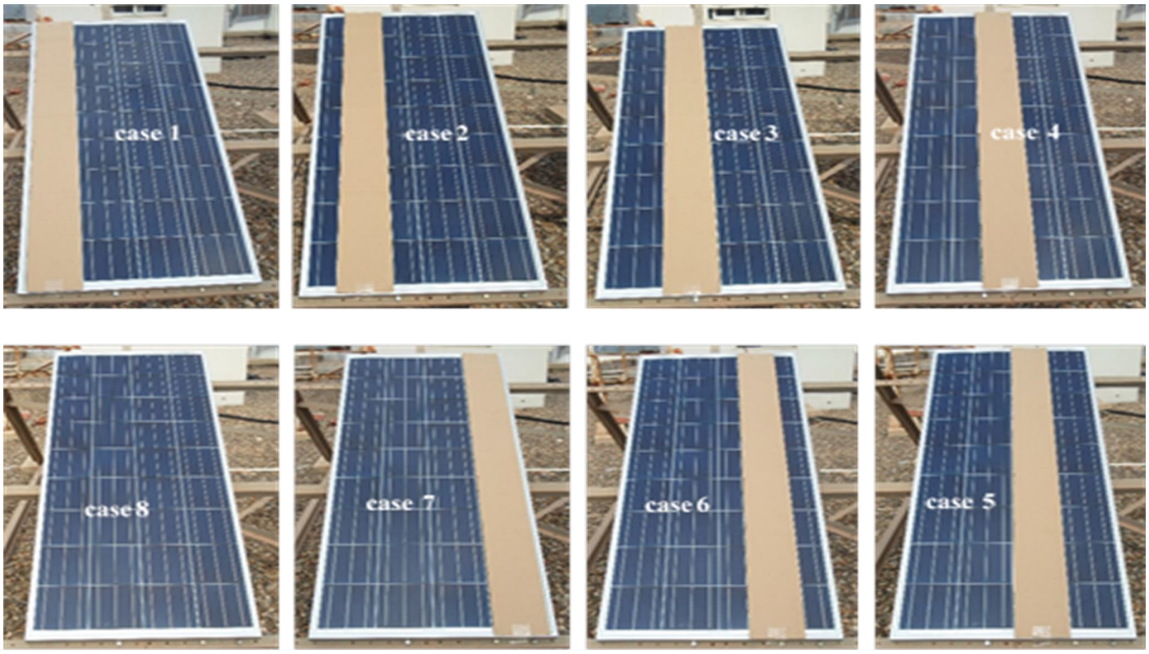

Figure 13. Shading positioning on the PV module.

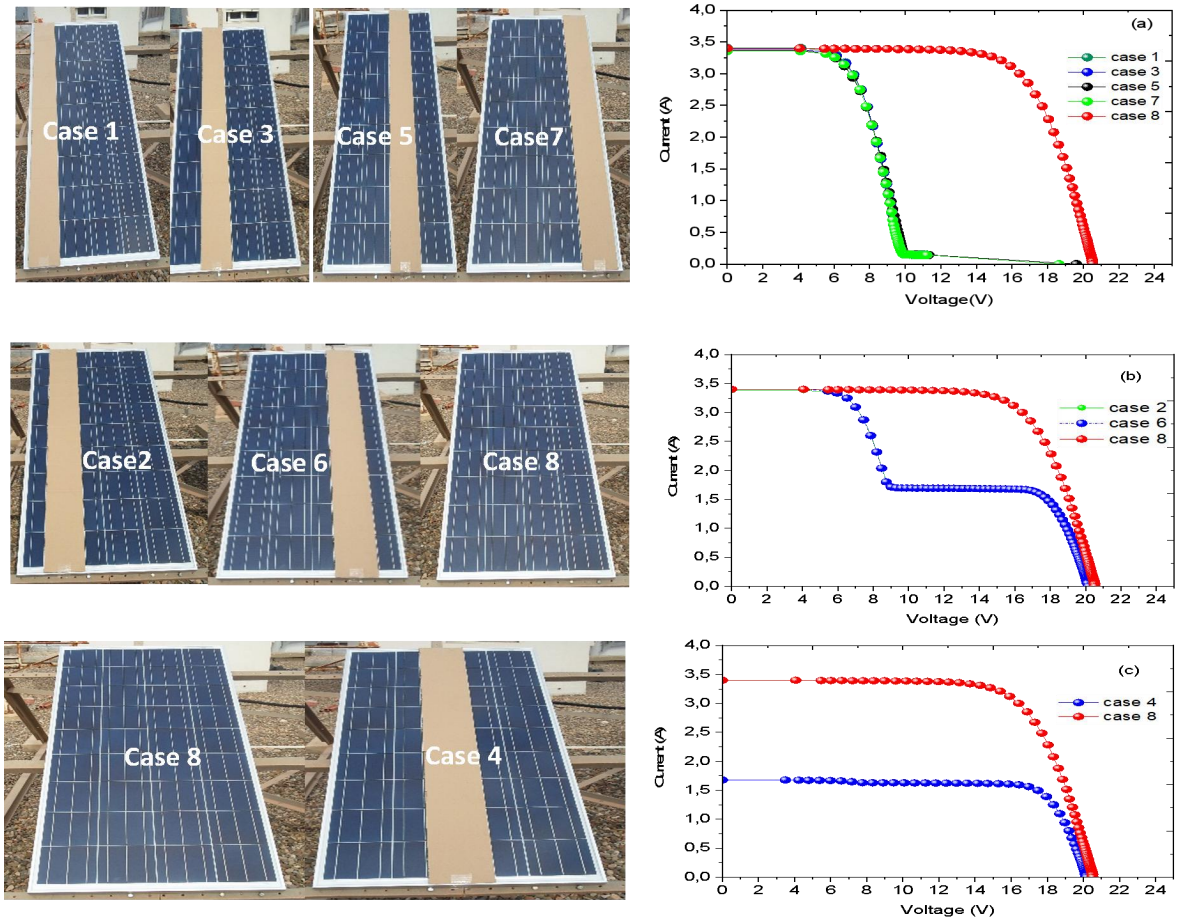

Figure 14. Vertical shading: a). 100% on half of a string, b). 50% on the whole of a string and c). 50% on half of two different strings.

3.3.2. Horizontal shading

The placement of horizontal shading on PV modules influences energy production, although the shape of the characteristic curve remains largely unchanged compared to vertical shading. While vertical shading can create significant irregularities in the power curve, horizontal shading does not visibly affect this curve, yet it greatly diminishes the performance of the modules.

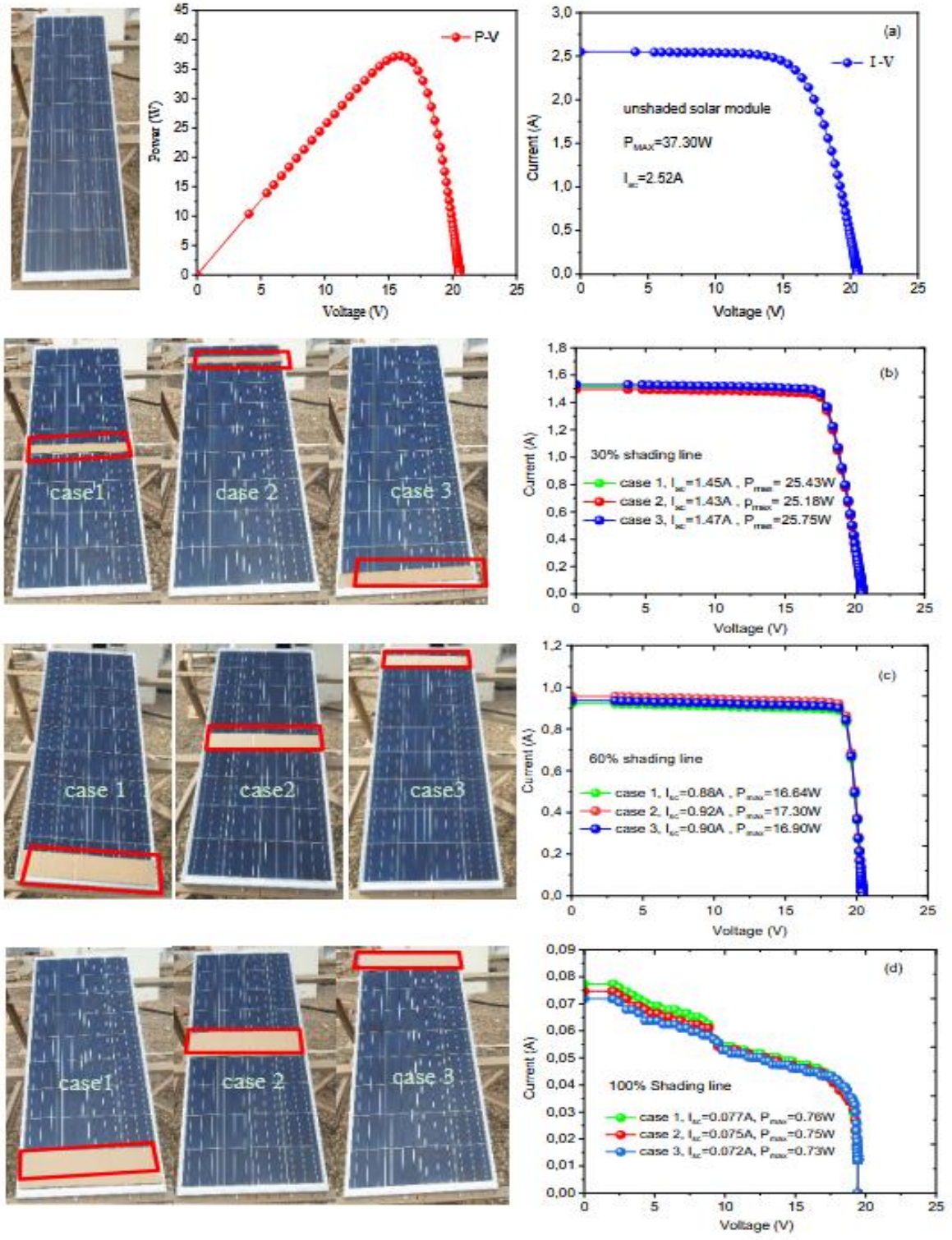

Figure 15. Horizontal shading: a) without shading b). A line shaded at 30%, c) A line shaded at 60%, and d).A line shaded at 100%.

The power loss is contingent upon the intensity of shading. For instance, the maximum power of a PV module without shading is around 49 W (see Figure 15. a). However, it is about 25W for 30% of shading on a PV module line, which represents a 49% reduction in power (see Figure 15. b). It is about 17W for 60% of shading on a PV, which represents a 67% decrease in power (see Figure 15. c). It is about 0.7 W for a 100% shaded line, which results in less than 1% of generated power (see Figure 15. d). These results demonstrate that horizontal shading has a direct and negative impact on the energy production of PV modules. In comparison to vertical shading, horizontal shading results in a significantly greater loss of generated power. This power degradation phenomenon occurs due to the considerable decline in the photo-generated current from the horizontally shaded cell. For instance, horizontal shading that covers 11% of the surface area of a PV module leads to an almost complete reduction in energy production (refer to Figure 15. d). In contrast, vertical shading, while covering 25% of the module area, results in a less significant power loss, with approximately 50% of the maximum power still available (see Figure 14. a). In conclusion, while horizontal shading does not directly influence the shape of the characteristic curve, but it has a significant negative impact on energy production. On the other hand, vertical shading, although it affects a larger portion of the surface, has a less dramatic effect on the efficiency of PV modules (Table 2).

Table 2. Electrical comparison between horizontal and vertical shading.

Shading type	Description	Effect on the *I-V* curve	Effect on the power	Figure
	Shading applied to groups of cells arranged in series in the same string.	*I-V* Curve with "stairs". Where: I_{sc}= 3.40A V_{oc}=19.61V *FF*= 31.90%	25% of shading product 50% pf power losses	*Figure 14. (a and b)*
Vertical	Shading applied to groups of cells arranged in series from 2 different string.	Continuous *I-V* curve Where: I_{sc}= 1.67A V_{oc}=20.18V FF=78.30%	25% of shading product 50% of power losses	*Figure 14. (c)*
horizontal	Shading applied horizontally across a row of cells	The form of the *I-V* curve remains largely unchanged. Where: I_{sc}= 0.074 A V_{oc}= 19.45V *FF*=51%	11% of shading leads to an almost total drop in power	*Figure 15. (c)*

4. Conclusion

Shading randomly affects PV systems, making their modeling complex and delicate, especially regarding electrical characteristics. This study aims to simplify simulation models of the electrical performance of PV systems, where it involved the development of a SIMULINK program designed to simulate the impact of bypass diodes on PV module performance in shaded environments. The program enables an examination of shading effects on the module's characteristic curves and

energy generation, while accounting for the function of bypass diodes that circumvent defective or shaded cells. Additionally, we performed experimental tests to analyze the impact of shading placement on the power output of the PV modules. The results revealed that horizontal shading causes substantial power losses far greater than those associated with vertical shading**.** Where horizontal covering of 11% of module surface leads to an almost total drop in energy production, however, vertical shading covering of 25% of module surface results in less severe power loss, with approximately 50% of maximum power remaining available. This emphasizes the necessity of managing shading effectively to optimize the performance of PV systems. These measurements were carried out in the Algiers region. The next measurements will take place in the Adrar, a desert region in Algeria.

Declarations

Availability of data and material: The datasets used and analyzed during the current study are available from the corresponding author on reasonable request.

Author contributions: AB,AA and ZS conceived and designed the research framework; AB,AA and ZS carried out the experimental and computational work; AA, ZS and MD provided critical guidance on the analytical methods and interpretation of results; AA,MD and SD performed the data analysis; AA, ZS and SD prepared the initial draft of the manuscript. All authors have read and approved the final manuscript. All authors contributed to editorial changes in the manuscript. All authors have participated sufficiently in the work and agreed to be accountable for all aspects of the work.

Acknowledgments: The authors would like to express their sincere gratitude to the Solar Equipment Development Unit (UDES) for the provision of material and human resources that contributed to the completion of this work.

Funding: This research received no external funding.

Conflicts of interest: The authors declare that they have no known competing financial interests or personal relationships that could have appeared to influence the work reported in this paper.

References

1. Ghimire, A.; Adhikari, B.; Pant, H.R.; Thapa, B.; Baral, B. Life cycle energy use and carbon emission of a modern single-family residential building in Nepal. *Current Research in Environmental Sustainability* 2024, 7, 100245. https://doi.org/10.1016/j.crsust.2024.100245
2. Wongmahasiri, R.; Wongvorachan, T.; Thampanichwat, C.; Phusakulkajorn, W. Impact of wall paint solar absorptance on CO_2 emissions in residential buildings: A case study from Bangkok. *Buildings* 2024, 14(12), 3958. https://doi.org/10.3390/buildings14123958
3. Harrison, A.; Farh, H.M.H.; Al-Shamma'a, A.A.; Mekhilef, S. An intelligent environmental-sensorless model for real-time optimization in photovoltaic-energy systems: Fast computation, long-term performance, and experimental validation. *Case Studies in Thermal Engineering* 2025, 74, 106818. https://doi.org/10.1016/j.csite.2025.106818
4. Harrison, A.; Mbasso, W.F.; Dagal, I.; Alombah, N.H.; Jangir, P.; Al-Gahtani, S.F. Environmental sensor-less hybrid analytical-machine learning (ESHAML) framework for ultra-fast solar irradiance estimation in climate-sensitive real-time applications: Experimental validation. *Measurement* 2025, 257, 118635. https://doi.org/10.1016/j.measurement.2025.118635
5. Zhang, H.; Seal, S.; Wu, D.I. Building energy management with reinforcement learning and model predictive control: A survey. *IEEE Access* 2022, 10, 27853 – 27862. https://doi.org/10.1109/ACCESS.2022.3156581
6. Bayasgalan, A.; Park, Y.S.; Koh, S.B.; Son, S. Comprehensive review of building energy management models: Grid-interactive efficient building perspective. *Energies* 2024, 17(19), 4794. https://doi.org/10.3390/en17194794

7. Mariano-Hernández, D.; Hernández-Callejo, L.; Zorita-Lamadrid, A.; Duque-Pérez, O.; Santos García, F. A review of strategies for building energy management system: Model predictive control, demand side management, optimization, and fault detect & diagnosis. *Journal of Building Engineering* 2021, 33, 101692. https://doi.org/10.1016/j.jobe.2020.101692
8. Smara, Z.; Aissat, A.; Deboucha, H.; Rezk, H.; Mekhilef, S. An enhanced global MPPT method to mitigate overheating in PV systems under partial shading conditions. *Renewable Energy* 2024, 234, 121187. https://doi.org/10.1016/j.renene.2024.121187
9. Smara, Z.; Aissat, A. Investigation of the relationship between shaded cell temperature and the operating point of PV systems. *Environmental Research, Engineering and Management* 2024, 80(2), 133–143. https://doi.org/10.5755/j01.erem.80.2.35188
10. Kunz, O.; Evans, R.J.; Juhl, M.K.; Trupke, T. Understanding partial shading effects in shingled PV modules. *Solar Energy* 2020, 202, 420–428. https://doi.org/10.1016/j.solener.2020.03.032
11. Witteck, R.; Siebert, M.; Blankemeyer, S.; Schulte-Huxel, H.; Köntges, M. Three bypass diodes architecture at the limit. *IEEE Journal of Photovoltaics* 2020, 10(6), 1828 – 1838. https://doi.org/10.1109/JPHOTOV.2020.3021348
12. Dhimish, M. 70% decrease of hot-spotted photovoltaic modules output power loss using novel MPPT algorithm. *IEEE Transactions on Circuits and Systems II: Express Briefs* 2019, 66(12), 2027–2031. https://doi.org/10.1109/TCSII.2019.2893533
13. Dhimish, M. Assessing MPPT techniques on hot-spotted and partially shaded photovoltaic modules: Comprehensive review based on experimental data. *IEEE Transactions on Electron Devices* 2019, 66(3), 1132–1144. https://doi.org/10.1109/TED.2019.2894009
14. Pillai, D.S.; Rajasekar, N. A comprehensive review on protection challenges and fault diagnosis in PV systems. *Renewable and Sustainable Energy Reviews* 2018, 91, 18 – 40. https://doi.org/10.1016/j.rser.2018.03.082
15. Chen, Z.; Chen, Y.; Wu, L.; Cheng, S.; Lin, P. Deep residual network based fault detection and diagnosis of photovoltaic arrays using current-voltage curves and ambient conditions. *Energy Conversion and Management* 2019, 198, 111793. https://doi.org/10.1016/j.enconman.2019.111793
16. Yadav, A.S.; Pachauri, R.K.; Chauhan, Y.K.; Choudhury, S.; Singh, R. Performance enhancement of partially shaded PV array using novel shade dispersion effect on magic-square puzzle configuration. *Solar Energy* 2017, 144, 780 – 797. https://doi.org/10.1016/j.solener.2017.01.011
17. Ramírez-Quiroz, F.A.; González-Montoya, D.; Bolaños-Martínez, F.; Ramos-Paja, C.A.; Camarillo-Peñaranda, J.R. Reconfiguración de arreglos fotovoltaicos basada en algoritmo genético. *Revista Facultad de Ingeniería Universidad de Antioquia* 2015, 75, 95 – 107. https://doi.org/10.17533/udea.redin.n75a10
18. Díaz-Dorado, E.; Cidrás, J.; Carrillo, C. Discrete I–V model for partially shaded PV arrays. *Solar Energy* 2014, 103, 96–107. https://doi.org/10.1016/j.solener.2014.01.037
19. Restrepo-Cuestas, B.J.; Durango-Flórez, M.; Trejos-Grisales, L.A.; Ramos-Paja, C.A. Analysis of electrical models for photovoltaic cells under uniform and partial shading conditions. *Computation* 2022, 10(7), 111. https://doi.org/10.3390/computation10070111
20. Bishop, J.W. Computer simulation of the effects of electrical mismatches in photovoltaic cell interconnection circuits. *Solar Cells* 1988, 25(1), 73 – 89. https://doi.org/10.1016/0379-6787(88)90059-2
21. Vieira, R.G.; de Araújo, F.M.U.; Dhimish, M.; Guerra, M.I.S. A comprehensive review on bypass diode application on photovoltaic modules. *Energies* 2020, 13(10), 2472. https://doi.org/10.3390/en13102472